TITLE

Applying 3D texture algorithms on MRI to evaluate quality traits of loin

AUTHORS

Mar Ávila[1], Daniel Caballero[2], Teresa Antequera[2], María Luisa Durán[1], Andrés Caro[1], and Trinidad Pérez-Palacios[2]*.

[1] Department of Computer Science, Research Institute of Meat and Meat Product (IproCar), University of Extremadura. Av/ Universidad, 10.003, Cáceres (Cáceres, Spain).

[2] Department of Food Technology, Research Institute of Meat and Meat Product (IproCar), University of Extremadura. Av/ Universidad, 10.003, Cáceres (Cáceres, Spain).

* Corresponding author. Tel.: +34 927-257-123. Fax: +34 927-257-110. E-mail address: triny@unex.es

ABSTRACT

This study firstly proposed the use of 3D MRI images to analyse loins in a non-destructive way. For that, interpolation and reconstruction techniques are applied on 2D MRI images of loins and the computational texture algorithms were adapted to analyse the obtained 3D images. The influence of the i) MRI acquisition sequences (Spin Echo (SE), Gradient Echo (GE), Turbo 3D (T3D)), ii) 3D texture features algorithms (GLCM, NGLDM, GLRLM, GLCM + NGLDM + GLRLM), and iii) regression techniques (Multiple Linear Regression (MLR), Isotonic Regression (IR)) was also evaluated. Combinations of SE or GE with any texture algorithm and any regression technique gave accurate results, with correlation coefficients higher than 0.75 and mean absolute error lower than 2. However, considering not only the accuracy of the methodology but also the computational cost, the use of GE, GLCM and IR could be proposed to determine physico-chemical parameters of loins non-destructively.

KEYWORDS

3D texture features; prediction; physico-chemical characteristics; loin.

INTRODUCTION

The evaluation of quality of meat products has been the subject for a great quantity studies for decades. In most cases, physico-chemical characteristics, such as colur, content of moisture, lipid, protein or salt content in fresh and dry-cured meat products, have been evaluated by means of destructive techniques, which also involve the use of organic solvents and take long time (Alasvand et al., 2012).

Magnetic Resonance Imaging (MRI) and computer vision techniques have emerged as ones of the alternative methodologies to the physico-chemical analysis, due to its non-destructive, non-invasive, non-intrusive, non-ionizing and innocuous nature. Several works aimed to determine quality characteristics of meat products by MRI have been published, most of them centred on loin and hams. The image acquisition has been carried out by using high field scanners (1.5 T) in most studies, e.g. in Iberian dry-cured loins of different sensory qualities (Cernadas et al., 2005), in fresh and dry-cured hams from Iberian pigs fattened different diets (Pérez-Palacios et al., 2010a; 2014), detecting the muscle and fat in pig carcasses (Monziols et al., 2006), throughout the processing of Iberian ham (Antequera et al., 2007; Caballero et al., 2016a; 2016b; Caro et al., 2001), S. Daniele hams (Manzoco et al., 2013). However, low field scanners (0.18-0.2 T) have also been used for MRI acquisition in some meat products: during the maturing process of Parma hams (Fantazzini et al., 2009) in dry-cured stuffed boned shoulders from Iberian pigs (Antequera et al., 2015), in fresh and dry-cured Iberian ham and loins (Ávila et al., 2015a; 2015b; Caballero et al., 2016a; 2016b; 2017a; Pérez-Palacios et al., 2014; 2015; 2017). Some of these studies carried out with low-field scanners have also indicated the importance of the acquisition sequence of MRI (Caballero et al., 2016a; 2016b, 2017a; Pérez-Palacios et al., 2017).

Once the MRI images are acquired, the following step consists on the MRI analysis, in order to obtain numerical data that can be further processed. For that, there are many algorithms of computer vision: for image segmentation, for texture feature extraction, for patterns recognition, etc. (Venkatramana and Jayachandra, 2010). Focusing on texture features extraction, classical 2D algorithms have been usually applied for analyzing MRI from meat products (Caballero et al., 2016a; 2016b; Cernadas et al., 2005; Kitanowski et al., 2012; Pérez-Palacios et al., 2011).

Results obtained in these studies using 2D-algorithms are reasonably good, however, the study of volumetric 3D structures could be a step forward, offering new possibilities (Melado-Herreros et al., 2013). Real world is not flat images but is three-dimensional. Therefore, there is loss of information when working with 2D images, while working with 3D images means trying to get all information within the images. Studies focused on 3D images are getting interest, finding some examples in the field of medicine, mostly for tumour detection and classification (Arunadevi and Nachimuthu, 2013; Madabhushi et al., 2003). Nevertheless, few examples on 3D images have been found. 3D reconstructions models of meat were reached by (Ávila et al., 2007; Goñi et al., 2008), in order to generate a geometry database saving efforts and decreasing error associated to experimental measurements. More recently, a new 3D algorithm has been proposed to study the distribution of textures in 3D images of loin from different orientations (Ávila et al., 2015a). The application of this 3D algorithm has allowed determining some sensory attributes of loin non-destructively (Ávila et al., 2015b). Other authors have also calculated the weight of broiler chickens using 3D computer vision (Krogh et al., 2016).

Following with the procedure for determining quality parameters of meat by means of MRI, last step consists of analyzing the numerical data given by the algorithm of computer vision. At this respect, currently, there is a growing interest in data mining. It is related to large data, being within a larger process known as Knowledge Discovery in Databases (KDD) (Fayyad et al., 1996). Its principal task is extracting hidden information from a large data set, by automatic or semi-automatic analysis, allowing interesting and previously unknown patterns (Hastie et al., 2001). These patterns are seen as summary of the input data, and can be groups of data records (cluster analysis), unusual records (anomaly detection) and dependencies among data (association rules). The goodness of data mining can be mainly ascribed to the rapidly decreasing cost of large storage device and the increasing ease in data collection over networks (Mitchell, 1999). The application of MRI-computer vision techniques based on 2D algorithm and data mining have allowed analyzing some physico-chemical and sensory parameters of loin and ham (Caballero et al., 2016a; 2016b; 2017a; Pérez-Palacios et al., 2014; 2017). However, there are no studies applying data mining on 3D algorithm for MRI analysis.

This works aims to i) interpolate new images in the gaps between the multi-slices ones to obtain 3D volumes, ii) adapt computational texture algorithms to analyze the obtained 3D reconstructed MRI, and iii) determine physico-chemical characteristics of meat products non-destructively, based on this new 3D approach by means of data mining.

MATERIAL AND METHODS

Material

Ten Iberian pork loins were used in this work (five fresh loins and five dry cured loins). Loins were acquired from Montesano (Jerez de los Caballeros, Spain). Average weight for fresh and dry-cured loin was around 3.5 kg and 1.4 kg, respectively.

Dry-cured Iberian loins were processed according to a traditional dry-curing method: loins were seasoned with a pickling sauce made of (per kg of raw loin): 22g salt, 5g sweet paprika, 3g hot-sweet paprika, 3g garlic and 6g of a commercial mixture (sodium chloride, sucrose, sodium ascorbate, sodium citrate, sodium nitrite and potassium nitrate), and subsequently kept for 3 days at 3° C to allow seasoning mixture uptake. Thereafter, loins were stuffed into collagen casings and held for 90 days at 6° C with a relative humidity around 85%.

GENERAL PROCEDURE

Figure 1 shows the general procedure design followed in this work. Iberian loins were MRI scanned, testing three multi-slice acquisition sequences. Firstly, an interpolation method was applied for three-dimensional reconstruction. The 3D images obtained were analyzed by means of three computational texture analysis algorithms. Then, the loins were physico-chemically analyzed, data obtained by means of physico-chemical analysis and MRI 3D texture analyses were grouped in a numerical database. Finally, prediction techniques of data mining were applied on that database, in order to obtain prediction equations for the physico-chemical parameters as a function of 3D computational texture features.

PHYSICO-CHEMICAL ANALYSIS

Fresh and dry-cured loins were analysed measuring the moisture (AOAC, 2000; reference 935.29), lipid content (Pérez-Palacios et al., 2008), water activity and instrumental colur. For the water activity, the system LabMaster-aw (NOVASINA AG, Lachen, Switzerland) was used after calibration. Instrumental colur was measured using a Minolta CR-300 colurimeter (Minolta Camera Corp., Meter Division. Ramsey, NJ) with illuminant D65, a 0° standard observer and a 2.5 cm port/viewing area. The following colur coordinates were determined: lightness (L), redness-greenness (a*) and yellowness-blueness (b*). The colurimeter was standardized before use with a white tile having the following values: L=93.5, a*=1.0 and b*=0.8. Salt content (AOAC, 2000; reference 971.19) was also determined in dry-cured loins.

IMAGE ACQUISITION

MRI images were generated at the ‘‘Animal Source Foodstuffs Innovation Services” (SiPA) of University of Extremadura (Caceres, Spain). A low field MRI scanner (ESAOTE VET-MR E-SCAN XQ 0.18 T) with a hand/wrist coil was used. Three different sequences of T1 were tested: spin echo (SE), gradient echo (GE) and turbo 3D (T3D). T1-weighted sequences have been used due to these MRI images are adequate for the application of computational texture algorithms. Eight different configurations of the parameters were used for SE, eight configurations for GE and eleven for T3D. Table 1 show in detail the selected values for each of the parameters.

In GE, the MR signal is refocused by inverting the gradient instead of using a 180° radiofrequency pulse. GE sequences are characterized by a strong signal-to-noise ratio.

In SE, a 90° radiofrequency excitation pulse is followed by a 180° radiofrequency refocusing pulse to reduce the effect of field inhomogeneity.

The T3D sequence is a GE sequence in which a special second encoding in the direction of the selection gradient enables 3D reconstruction. The signal-to-noise ratio is also high in this type of sequence.

The MRI acquisition was done at 23 °C. All the images were in DICOM format, with a 256 x 256 resolution, and 256 grey levels.

INTERPOLATION AND 3D RECONSTRUCTION

A 3D image is reconstructed using all MRI slices obtained of each loin with each configuration of each acquisition sequences. This is done by linear interpolation methods, using VTK (Visualization Toolkit). It is a set of free code libraries for the visualization and processing of images, such as the creation of graphic objects in 2D and 3D (http://www.vtk.org/).

Once the 3D images have been obtained, they will be analyzed by using several texture algorithms.

Figure 2 shows images from different MR sequences with their corresponding interpolation and 3D reconstruction.

TEXTURE ANALYSIS

Firstly, on each image, a central area with 20 x 20 pixels was selected, which is called Region of Interest (ROI). The ROI is the area inscribed in the same spatial situation in all MRI. ROIs of each loin were reconstructed in three dimensions. In total, 270 three-dimensional images were used (270 loins reconstructed in three dimensions), given that the number of configurations for each sequence (8, 8 and 11 for SE, GE and T3D, respectively) and the number of loins (10).

Then, three classical algorithms for texture analysis were adapted to work with three-dimensional images and be applied on 3D images of loins, as described below. While classical algorithms use four orientations to obtain the texture features (figure 3a), 3D algorithms use the thirteen orientations (figure 3b) available in their structural space. The darkest pixel of each grid can be considered the referent. When working on two-dimensional images only four directions are considered (horizontal, vertical and two diagonal orientations), however, when working in three-dimensional space some more orientations can be considered.

The grey level co-occurrence matrix, GLCM (Haralick et al., 1973), is based on the estimation of the second-order joint conditional probability density functions, $P(m, n, d, a)$. Each $P(m, n, d, a)$ is the probability of moving from grey level m to grey level n, provided that the spacing between pixels is d and the orientation is given by a. If an image has Ng grey levels, then the GLCM can be written as the addition of Ng x Ng matrices, one for each for the orientations. The number of matrices will depend on the orientations that are taken into account. Each matrix is calculated by counting the number of times each pair of grey levels (m, n) occurs at the separation d and in the direction a. We assume $d= 1$. In the case of 2D images the orientations on which the matrix is calculated are 4: *0º-180º, 45º-225º, 90º-270º* and *135º-315º*, as it can be seen in figure 3a. In our proposal, for the 3D images, the matrices are calculated according to 13 orientations: *0º-180º, 90º-270º, 135º-315º, 45º-225º* in the *XY* plane, *0º-180º, 135º-315º, 45º- 135º - 315º, 45º - 225º* in the *XZ* plane and *135º,* *315º, 45º, 225º* in the *XYZ* plane, as can be seen in figure 3b. For the 13 orientations, the coocurrence matrix of grey levels has been computed in one direction, in order to avoid repeating the cooccurrence computations in the opposite directions (the other 13 orientations). Following it is added to each cooccurrence matrix its transposed matrix, having the 26 orientations.

In this way, the images are being analyzed in all possible directions so that all information is considered. Subsequently, these thirteen matrices are added to obtain a final GLCM with some degree of rotation invariance.

Finally, a vector of 10 features is obtained. It is common to use derived features defined by Haralick et al. (1973): ENE (Energy), ENT (Entropy), COR (Correlation), HC (Haralick's correlation), IDM (Inverse difference moment), INE (Inertia), CS (Cluster shade), CP (Cluster prominence), CON (Contrast) and DIS (Dissimilarity).

Neighborhood grey level dependence matrix (NGLDM) provides rotation invariant features, by considering the relationship between an element and all its neighbor elements at one time instead of one direction at a time. This eliminates the angular dependency, while at the same time reduces the calculation required to process an image. It is based on the assumption that a grey level spatial dependence matrix of an image can adequately specify this texture information (Siew et al., 1988). In our 3D proposal, the neighborhood is a cube, not only a plane rectangular area. So, the relationships between the central voxel and its neighbors are analyzed, in the same thirteen angular directions indicated before. One more time one matrix for a 3D image is obtained.

The usual numerical measures on this matrix are: SNE (Small number emphasis), LNE (Large number emphasis), NNU (Number non-uniformity), SM (Second moment), ENT (Entropy).

Grey level run length matrix (GLRLM) (Galloway et al., 1975), which is a method based on measuring runs of grey levels in the image. A run is a set of consecutive pixels in the image having the same grey-level value. This method involves the counting runs length (the number of consecutive pixels with the same grey level in a particular orientation). In our proposal, for the 3D images, the orientations are 13: *0º-180º, 90º-270º, 135º-315º, 45º-225º* in the *XY* plane, *0º-180º, 135º-315º, 45º- 135º - 315º, 45º - 225º* in the *XZ* plane and *135º, 315º, 45º, 225º* in the *XYZ* plane.

A large number of straight pixels with the same grey level represent a coarse texture, a small number of these pixels represent a fine texture. So, the lengths of these texture primitives in different spatial directions can serve as texture description. From this method, the features being applied are: SRE (Short run emphasis), LRE (Long run emphasis), GLNU (Grey level non-uniformity), RLNU (Run length non-uniformity), RPC (Run percentage), LGRE (Low grey-level run emphasis), HGRE (High grey-level run emphasis), SRLGE (Short run low grey-level emphasis), SRHGE (Short run high grey-level emphasis), LRLGE (Long run low grey-level emphasis), LRHGE (Long run high grey-level emphasis) (Siew et al., 1988; Sonka et al., 1999).

Each method (GLCM, NGLDM, GLRLM) was applied individually and altogether (GLCM + NGLDM + GLRLM), obtaining feature vectors with 10, 5, 11, and 26 computational texture features, respectively.

PREDICTIVE TECHNIQUES

The free software WEKA (Waikato Environment for Knowledge Analysis) (http://www.cs.waikato.ac.nz/ml/weka/) was used for carrying out the predictive techniques of data mining.

Two correlation techniques have been applied for the prediction experiments, multiple linear regression (MLR) and isotonic regression (IR). MLR is the most common technique of linear regression analysis. It is used to explain the relationship between one dependent variable from independent variables. This technique gives a linear regression equation, which can be used to predict future values (Hastie et al., 2001). The M5 method of attribute selection and a ridge value of 1×10^{-4} were applied. It is based on stepping through the attributes, being the one with the smallest standardized coefficient removed until no improvement is observed in the estimation of the error.

When the values of the database are highly correlated, the use of non-linear regression is recommended. In these cases, the IR is considered as a good option. It provides a set of values from the information stored on a database. It is based on estimating ordered values for a dependent variable (i.e. moisture) as a function of one of the input parameters. Only the input parameters providing better adjustment results will be selected. Finally, an interpolation function is established (polynomial trend line) to compare the provided set data with original values in the database, obtaining the prediction equation (Barlow et al., 1972; Borge, 1985).

The correlation coefficient (R) was used for evaluating the goodness of fit of the prediction according to the rules given by Colton (Colton, 1974), who considered that a correlation coefficient from 0 to 0.25 indicates little to no relationship; from 0.25 to 0.50 indicates a weak relationship; from 0.50 to 0.75

indicates a moderate to good relationship; and from 0.75 to 1 indicates a very good to excellent relationship.

Additionally, the mean absolute error (MAE) (Hyndman and Koehler, 2006a) was used to validate the prediction results too. The MAE measures the difference between real values and predicted ones. Values of MAE less than 2 are appropriate (Hyndman, 2006b). It is calculated by the following equation:

STATISTICAL ANALYSIS

One-way analysis of variance (ANOVA) of the General Linear Model (GLM) was used i) to evaluate the effect of the MRI sequence acquisition on the values of the computational texture features and ii) to validate the prediction results by comparing real and predicted values of the physico-chemical characteristics. Analyses were done by using the SPSS package (v.20.0) (IBM Co., New York, New York, U.S.A.).

RESULTS AND DISCUSSION

RESULTS ON PHYSICO-CHEMICAL ANALYSIS OF LOINS

In fresh loins, percentage of moisture and lipid were 65.55 ± 1.82 and 12.78 ± 1.36%, respectively, and the water activity was 0.98 ± 0.00. The colur coordinates, L, a*, and b* were, respectively, 55.32 ± 3.12, 12.92 ± 0.69, and 5.58 ± 0.72. In comparison to fresh loins, in dry-cured loins lower values of moisture and water activity were found (32.22 ± 2.96% and 0.86 ± 0.00, respectively). This is due to the dry-curing process. And, consequently, the lipid content increased (21.61 ± 6.84%) in dry-cured loins. Similar findings have been previously reported (Estevez et al., 2004; Muriel et al., 2004; Ramírez and Cava, 2007; Utrilla et al., 2010). Analyzing the colur coordinates in dry-cured loins: L decreased (40.61 ±

4.44), as consequence of the desiccation process; a* and b* increased (15.31 ± 1.60 and 8.04 ± 1.48, respectively), which could be also ascribed to the water losses that lead to a higher pigment concentration, and therefore to the redder and more vivid colur (Perez-Palacios et al., 2011).

EFFECT OF SEQUENCE ACQUISITION ON 3D MRI

Figure 2 shows 2D MR images of loins acquired by different sequence acquisition, SE, GE and T3D and the respective 3D reconstructions obtained from these images. Some visual differences can be appreciated depending on the sequence acquisition. In 2D images, intramuscular fat is represented by the white colur and the lean is illustrated by the grey color. In general, SE offered images that are sharper and better defined than those obtained by GE and T3D acquisition sequences. This effect of the sequence acquisition of MRI has been previously reported in (Caballero et al. 2017a; Pérez-Palacios et al. 2017).

Once the 3D images of loins were reconstructed, they were analyzed by three computational texture algorithm previously adapted to 3D images. Table 2 shows the average values of all 3D computational texture features from MRI of loins acquired with different sequences. This finding is so remarkable, since it shows the goodness of the interpolation and 3D reconstruction procedures and of the modified texture analysis algorithms, and let it evaluate the influence of the acquisition sequence on the values of the 3D texture features. As can be observed in table 2, SE obtained the highest values for Energy, Correlation, IDM, LNE, SM, LRE, GLRE, LRLGE and LRHGE, while the highest levels of HC, Contrast, ENT, SER, HGRE and SRHGE were found in GE, and, in T3D, Entropy, Inertia, CS, CP, Dissimilarity, SNE, NNU, GLNU, RLNU, RPC and SRLGE showed the highest values. The computational texture features have been related to some properties of the images (Ávila et al., 2015a; Mohanty et al., 2011; Murali et al., 2011). Energy and NNU measure the uniformity of the images, Entropy and SM, the complexity, IDM and ENT, the homogeneity, SNN the fineness, and LNE the roughness. Correlation, HC and Inertia are associated to the grey level of the pixels. The symmetry of the images and of the grey levels are related to CS and CP, respectively. Contrast and Dissimilarity yield measurement of the contrast and the differences among the grey levels of the image. SER, LRE and RPC are associated to the quantity and size of the runs. GLNU and RLNU depend on the equitable distribution of the runs, and LGRE and GLRE on the high and low grey levels distribution. SRLGE y SRHGE are associated to long runs and LRHGE and LRLGE to big runs.

These semantic approximation between computational texture features and properties of the images could be considered to explain some differences due to the sequence acquisition. Images from SE seems to be rougher and less fine than those from T3D, since LNE, which measures the roughness of the images, showed the highest values in SE, and SNE, which is related to the fineness of the images, obtained the highest values in T3D. In T3D images, the runs should not be distributed equitably, due to the highest values for GLNU and RLNU when this sequence acquisition is applied. And big runs should be found in SE images, because of this sequence acquisition obtained the highest values of LRHGE and LRLGE.

PREDICTION OF PHYSICO-CHEMICAL CHARACTERISTICS OF LOIN AS A FUNCTION OF 3D TEXTURES FEATURES

The physico-chemical parameters related to the loin quality were predicted from the 3D texture features by using: a) three sets of 3D images acquired with different sequences (SE, GE and T3D), b) different texture algorithms (GLCM, NGLDM, GLRLM, GLCM+NGLDM+GLRLM) and c) different predictive techniques (MLR, IR). Therefore, the discussion focuses on determining the best combination of sequence of image acquisition, algorithm of 3D texture features and prediction technique.

Thus, for each physico-chemical parameter, twenty-four prediction equations were obtained (3 acquisition sequence x 4 computational texture algorithms x 2 predictive techniques). Tables 3 and 4 show the values of the correlation coefficients and MAE for the predictive analysis carried out by MLR and IR, respectively.

When using MLR, combination of SE and GE acquisition sequence with any computational algorithm (GLCM, NGLDM, GLRLM, GLCM+NGLDM+GLRLM) gave correlation values higher than 0.75 (very good to excellent correlation) and MAE values lower than 2 for most physico-chemical parameters. In the case of T3D, in general, correlation coefficient between 0.5 and 0.75 (moderate to very good correlation) and MAE lower than 2 were obtained in combination to any computational algorithm. Thus, initially, all studied combination of sequence acquisition, especially of SE and GE, with 3D algorithms could be appropriated.

Regarding to IR (Table 4), a similar trend than observed when using MLR was found. Generally, the combination of SE or GE with any algorithm of 3D MRI analysis (GLCM, NGLDM, GLRLM, GLCM+NGLDM+GLRLM) offered very good to excellent correlation coefficients ($R > 0.75$) and MAE values lower than 2. In the case of T3D in combination with any computational algorithm, moderate to very good correlation coefficient ($R = 0.5-0.75$) and MAE lower than 2 were obtained for most physico-chemical parameters. In this case, again, any combination of sequence acquisition, especially SE or GE, with any 3D algorithm could be initially applied.

3D approaches showed a higher accuracy, especially when using T3D acquisition sequence in comparison to prediction results on physico-chemical parameters of loins based on 2D texture features (Pérez-Palacios et al., 2017). This could be ascribed to the distance between slices that is lower in T3D than in SE and GE. Consequently, T3D obtains more information from MRI than the other sequences. Thus, when using classical texture features to analyse 2D MRI from T3D sequence acquisition, some information may be lost, however, in reconstructed 3D images all information is considered in a useful way. Moreover, other authors have also found better results using 3D than 2D images (Miklos et al., 2015).

Correlation coefficients and MAE values obtained by MLR and IR have also been compared. In general, no marked differences have been found in most physico-chemical parameters.

Thus, considering the prediction accuracy the following combinations of sequence acquisition - 3D texture algorithm – prediction technique of data mining could be used for prediction physico-chemical parameters of loins as a function of 3D texture features: SE - GLCM+NGLDM+GLRLM – MLR; SE - GLCM – IR; SE - NGLDM – IR; SE - GLRLM – IR; SE - GLCM+NGLDM+GLRLM – IR; GE - GLCM – IR; GE - NGLDM – IR; GE - GLRLM – IR; GE - GLCM+NGLDM+GLRLM – IR.

Taking a step forward regarding the best combination for prediction physico-chemical parameters of loins, apart from the accuracy in the determination, the sake of simplicity and the computational efficiency are also notable aspects that should be take into account. In regards to the MRI sequence acquisition, both SE and GE could be used. However, exploring on the results with more detail, it is noted that SE achieved slightly higher correlation coefficients and lower MAE than GE, when applying MLR. This can be ascribed to the better performance in terms of the signal-to-noise ratio of SE than GE and T3D, which are characterized by a strong signal-to-noise ratio and fast acquisition. However, in IR, SE and GE are so similar. In this case, the computational time (total time to acquire all MRI of one loin for each configuration of each acquisition sequence) should be considered, which is lower in GE (38 min) than in SE and T3D (50 and 58 min, respectively). As for the 3D texture algorithm, in the case of MLR, GLCM+NGLDM+GLRLM offered slightly better prediction results than GLCM, NGLCM and GLRLM. When using IR, GLCM could be selected as the best option. In terms of computational time, GLCM and GLRLM are more appropriate ($O(n^2)$) than NGLDM and GLCM+NGLDM+GLRLM ($O(n^3)$) (Caballero et al., 2017b). In relation to the predictive technique of data mining, which were comparable in terms of prediction results, MRI leads to two-order polynomial equations, with a number of independent variables (computational texture features), and IR leads to sixth-order equations with only one independent variable. Thus, MLR is simpler and requires less algorithm complexity, but the prediction equation of IR needs less computational data. The lineally dependence between data should also be considered. In fact, the application of IR is recommended when the values of the database are highly correlated (Perez-Palacios et al., 2014). Considering all these premises, it could be indicate the combination of GE with GLCM and IR for predicting physico-chemical parameters of loins as a function on 3D texture features from MRI with high accuracy and low computational complexity. A different option is indicated when using 2D texture features. In this case, the combination of SE acquisition sequence, GLCM method, and MLR seems to the best option (Pérez-Palacios et al., 2017).

MRI techniques allow for the detection of Hydrogen and other features like fat fluidity and water retention, which easily explains the accurate results for prediction moisture, water activity and lipid. In the case of colur coordinates and salt, some discussion is worth mention. Colur coordinates are mainly related to characteristics of fresh meat and changes during processing (water loss, myoglobin oxidation) (Perez-Palacios et al., 2011), and salt influences on the activity of muscle enzymes, water activity and protein solublization, and consequently on the texture and flavour of the final product (Toldrá et al., 1997). These chemical reactions could modify the relation of Hydrogen with other molecules, leading to a different response of Hydrogen in MRI and image texture parameters. In the same way. In addition, previous authors have shown that 1H MRI (Fantazzini et al., 2005, 2009; Caballero et al., 2017) is a suitable tool to investigate salt in inner layers of hams, finding that computational texture features are able to differentiate muscle with different salt content.

As example, Table 5 shows prediction equations for physico-chemical parameters of loins by applying IR on computational texture features of GLCM method from MRI acquired with GE sequence. As can be seen, moisture and water activity depend on IDM, lipid and L colur coordinate on HC, salt on CS and a* and b* colur coordinates on Energy. These associations between the physico-chemical parameters and the computational texture features could be ascribed to the properties of the images that are defined by the computational texture features. Thus, moisture and water activity would be associated to the homogeneity of the image, lipid and L, a* and b* colur coordinates to the grey level of the pixels and salt to the symmetry of the images. This can be an important contribution for the ''semantic gap" existing between the computational features and some biological terms, which has been previously claimed (Jian et al., 2009; Reyes et al., 2008; Pérez-Palacios et al., 2010b)

To validate the proposed prediction equations, real and predicted values of physico-chemical parameters were statistically compared (Table 6). As can be seen, no significant differences ($p>0.05$) were found for all physico-chemical parameters of both fresh and dry-cured loins. This finding reinforced the accuracy of this method. It is also worth noting the fact that the same prediction equations can be applied for predicting in fresh and dry-cured loins, which is more comfortable than having to use different equations for fresh and dry-cured products, as proposed previously in 2D images (Caballero et al., 2017a; Pérez-Palacios et al., 2017).

CONCLUSIONS

Interpolation and 3D reconstruction procedures as well as the adaptation of classical computational texture analysis algorithms to analyze 3D images described in this work allow i) analyzing MRI of fresh and dry-cured loins appropriately, and ii) carrying out predictive analysis of the physico-chemical parameters of loins.

The sequence acquisition of MRI of loins significantly influences the visual appearance of the 3D reconstructed MRI of loins, as well as the values of the 3D computational texture features.

It is possible to achieve prediction equations for the physico-chemical parameters of loins as a function of 3D computational texture features of MRI.

The accuracy of the prediction equations are principally influenced by the sequence acquisition of MRI, whereas the 3D algorithm and the predictive technique are not notable effects. However, these three factors have an effect on the computational cost of the prediction results.

Thus, in terms of accuracy, different combinations of sequence acquisition (SE or GE), 3D algorithm (GLCM, GLRLM, NGLDM, GLCM+NGLDM+GLRLM) and predictive technique (MLR, IR) can be used to determine physico-chemical parameters of fresh and dry-cured loins non-destructively. However, if the computational cost is also considered, the combination of GE – GLCM – IR seems to be the best option.

ACKNOWLEDGMENTS

The authors wish to acknowledge the funding received from the FEDER-MICCIN Infrastructure Research Project (UNEX-10-1E-402), Junta de Extremadura economic support for research group (GRU15173 and GRU15113) and we also wish to thank the Animal Source Foodstuffs Innovation Service (SiPA, Cáceres, Spain) from the University of Extremadura.

REFERENCES

Alasvand, S., Kadivar, M., Aminlari, M. and Shekarforoush, S. (2012). A comparative study of physico-chemical and functional properties, and ultrastructure of ostrich meat and beef during aging. CyTA - Journal of Food, 10(3), 201-209.

Antequera, T., Caro, A., Rodríguez, P.G. and Pérez-Palacios, T. (2007). Monitoring the ripening process of Iberian Ham by computer vision on magnetic resonance imaging. Meat Science, 76, 561–567.

Antequera, T., Caballero, D., Caro, A. and Pérez-Palacios, T. (2015). MRI to study the cohesion of dry-cured stuffed boned shoulders from Iberian pigs. In IV Farm Animal Imaging Conference. Edinburgh, United Kingdom.

Association of Official Analytical Chemist (2000). Official Methods of Analysis of AOAC International. Vols. 1 and 2, 17th edn. Ed. AOAC International. Gaithersburg, Maryland, U.S.A.

Arunadevi, B. and Nachimuthu, S. (2013). Texture analysis for 3D classification of brain tumor tissues. Przeglad Elektrotechniczny, 89, 338-342

Ávila, M.M., Durán, M.L., Antequera, T., Palacios, R. and Luquero, M. (2007). 3D reconstruction on MRI to analyse marbling and fat level in Iberian loin. Lecture Notes in Computer Science, 4477, 145-152.

Ávila, M.M., Caballero, D., Durán, M.L. and Antequera, T. (2015a). Computational 3D texture features to predict sensorial traits of Iberian loin based on MRI. In IV Farm Animal Imaging Conference. Edinburgh, United Kingdom.

Ávila, M.M., Caballero, D., Durán, M.L., Caro, A., Pérez-Palacios, T. and Antequera, T. (2015b). Including 3D-textures in a Computer Vision System to Analyze Quality Traits of loin. Lecture Notes in Computer Science, 9163, 456-465.

Barlow, R.E., Bartholomew, D., Bremner, J.M. and Brunk, H.D. (1972). Statistical Inferece Under Order Restriction: The Theory and Application of Isotonic Regression. Ed. Wiley, New York, New York, U.S.A.

Borge, L. (1985). Estimación y contrastes de hipótesis en el modelo lineal general con restricciones de desigualdad. Doctoral thesis. University of Valladolid, Valladolid, Spain.

Caballero, D., Antequera, T., Caro, A., Durán, M.L. and Pérez-Palacios, T. (2016a). Data Mining on MRI-Computational texture features to predict sensory characteristics in ham. Food Bioprocess Technology, 9, 699-708.

Caballero, D., Caro, A., Rodríguez, P.G., Durán, M.L., Ávila, M.M., Palacios, R., Antequera, T. and Pérez-Palacios, T. (2016b). Modeling salt diffusion in Iberian ham by applying MRI and data mining. Journal of Food Engineering, 189, 115-122.

Caballero, D., Antequera, T., Caro, A., Ávila, M.M., Rodríguez, P.G. and Pérez-Palacios, T. (2017a). Non-destructive analysis of sensory traits of dry-cured loins by MRI – Computer vision techniques and data mining. Journal of the science of food and agriculture, 97, 2942-2952.

Caballero, D., Caro, A., Ávila, M.M., Rodríguez, P.G., Antequera, T. and Pérez-Palacios, T. (2017b). New fractal features and data mining to determine food quality based on MRI. IEEE Latin American Transactions, 15(9), 1778-1785.

Caro, A., Rodríguez, P.G., Cernadas, E., Durán, M.L. and Villa, D. (2001). Applying active contours to muscle recognition in Iberian ham MRI. In: IASTED International Conference Signal Processing, Pattern Recognition and Applications, Rhodes, Greece.

Cernadas, E., Carrión, P., Rodriguez, P.G., Muriel, E. and Antequera, T. (2005). Analyzing magnetic resonance images of Iberian pork loin to predict its sensorial characteristics. Computer Vision and Image Understanding, 98, 345-361.

Colton, T. (1974). Statistics in medicine. Ed. Little Brown and Co., New York, New York, U.S.A.

Estevez, M., Ventanas, J. and Cava, R. (2004). Lipolytic and oxidative changes during refrigeration of cooked loin chops from three lines of free-range-reared Iberian pigs slaughtered at 90 kg live weight and industrial genotype pigs. Food Chemistry, 87, 367–376.

Fantazzini, P., Bortolotti, V., Garavaglia, C., Gombia, M., Riccardi, S., Schembri, P., Virgili, R. and Bordini, C.S. (2005). Magnetic resonance imaging and relaxation analysis to predict non-invasively and non-destructively salt-to-moisture ratios in dry-cured meat. Magnetic Resonance Imaging, 23, 359–361.

Fantazinni, P., Gombia, M., Schembri, P., Simoncini, N. and Virgili, R. (2009). Use of magnetic resonance imaging for monitoring Parma dry-cured ham processing. Meat Science, 82, 219–227.

Fayyad, U., Piatetsky-Shapiro, G. and Smyth, P. (1996). From data mining to knowledge discovery in databases. AI Magazine, 17, 37–54.

Galloway, M.M. (1975). Texture classification using grey level run length. Computer graphics and image processing, 4, 172-179.

Goñi, S.M., Purlis, E. and Salvadori V.O. (2008). Geometry modelling of food materials from magnetic resonance imaging. Journal of Food Engineering, 88(4), 561-567.

Haralick, R.M., Shanmugam, K. and Dinstein, I. (1973). Textural features for image classification. IEEE Transactions on Man and Cybernetics, 3(6), 610-621.

Hastie, T., Tibshirani, R. and Friedman, J. (2001). The Elements of Statistical Learning: Data Mining. Inference and Prediction. Ed. Springer-Verlag, New York, New York, U.S.A.

Hyndman, R. and Koehler, A.B. (2006a). Another look at measures of forecast accuracy. International Journal of Forecasting, 22, 679-688.

Hyndman, R. (2006b). Another look at forecast accuracy metrics for intermittent demand. International Journal of Applied Forecasting, 4, 43-46.

Jian, M., Gou, H. and Liu, L. (2009). Texture image classification using visual perceptual texture features and gabor wavelet features. Journal of computers, 4, 763-770.

Kitanowski, I., Trojacanec, K., Dimitrovski, I. and Loskovska S. (2012). Modality classification using texture features. Advances in Intelligent and Soft Computing, 150, 189-198.

Krogh, A., Lisouski, P. and Ahrendt, P. (2016). Weight prediction of broiler chickens using 3D computer visión. Computers and Electronics in Agriculture 123, 319-326.

Madabhushi, A., Feldman, M., Metaxas, D., Chute, D. and Tomaszewski J. (2003). A novel stochastic combination of 3D texture features for automated segmentation of prostatic adenocarcinoma from high resolution MRI. Lecture Notes in Computer Science, 2878, 581-591.

Manzoco, L., Anese, M., Marzona, S., Innocente, N., Lagazio, C. and Nicoli, M.C. (2013). Monitoring dry-curing of S. Daniele ham by magnetic resonance imaging. Food Chemistry, 141, 2246–2252.

Melado-Herreros, A, Muñoz-García, M. A., Blanco, A., Val, J., Fernández-Valle, M. E. and Barreiro, P. (2013). Assessment of watercore development in apples with MRI: Effect of fruit location in the canopy. Postharvest Biology and Technology, 86, 125-133.

Miklos, R., Nielsen, M.S., Einarsdottir, H., Feidenhans'l, R. and Lametsch, R. (2015). Novel X-ray phase-contrast tomography method for quantitative studies of heat induced structural changes in meat. Meat Science, 100, 217-221.

Mitchell, T.M. (1999). Machine learning and data mining. Communications of the ACM, 42, 30–36.

Mohanty, A.K., Beberta, S. and Lenka, S.K. (2011). Classifying bening and malignant mass using GLCM and GLRLM based texture features from mammogram. International Journal of Engineering Research and Applications, 1, 687-693.

Monziols, M., Collewet, G., Bonneau, M., Mariette, F., Davenel, A. and Kouba, M. (2006). Quantification of muscle, subcutaneous fat and intramuscular fat in pig carcasses and cuts by magnetic resonance imaging. Meat Science, 72, 146-154.

Murali, A., Moss, R.H. and Stoecker, W.V. (2011). Detection of pigment network in dermatoscopy images using texture analysis. Computerized medical imaging and graphics, 28, 225-234.

Muriel, E., Ruiz, J., Martin, D., Petron, M.J. and Antequera, T. (2004). Physico-chemical and sensory characteristics of dry-cured loin from different Iberian pig lines. Food Science Technology International, 10, 117–123.

Pérez-Palacios, T., Ruiz, J., Martin, D., Muriel, E. and Antequera T. (2008). Comparison of different methods for total lipid quantification. Food Chemistry, 110, 1025-1029.

Pérez-Palacios, T., Antequera, T., Durán, M.L., Caro, A., Rodríguez, P.G. and Ruiz, J. (2010a). MRI-based analysis, lipid composition and sensory traits for studying Iberian dry-cured hams from pigs fed with different diets. Food Chemistry, 126, 1366–1372.

Pérez-Palacios, T., Antequera, T., Molano, R., Rodríguez, P.G. and Palacios, R. (2010b). Sensory traits prediction in dry-cured hams from fresh product via MRI and lipid composition. Journal of Food Engineering, 101, 152-157.

Pérez-Palacios, T., Antequera, T., Durán, M.L., Caro, A., Rodríguez, P.G. and Palacios, R. (2011). MRI-based analysis of feeding background effect on fresh Iberian ham. Food Chemistry, 126, 1366-1372.

Pérez-Palacios, T., Ruiz, J., Martín, D., Barat, J.M. and Antequera, T. (2011). Pre-cure freezing effect on physiochemical, texture and sensory characteristics of Iberian ham. Food Science and Technology International, 17, 127-133.

Pérez-Palacios, T., Caballero, D., Caro, A., Rodríguez, P.G. and Antequera, T. (2014). Applying data mining and Computer Vision Techniques to MRI to estimate quality traits in Iberian hams. Journal of Food Engineering, 131, 82-88.

Pérez-Palacios, T., Caballero, D., Caro, A. and Antequera, T. (2015). Low-field Magnetic Resonance Imaging and computational texture features to predict moisture and lipid content of loins. In IV Farm Animal Imaging, Edinburgh, United Kingdom.

Pérez-Palacios, T., Caballero, D., Antequera, T., Durán, M.L., Ávila, M.M. and Caro, A. (2017). Optimization of MRI acquisition and texture analysis to predict physico-chemical parameters of loins by data mining. Food Bioprocess Technology, 10, 750-758.

Ramírez, M.R. and Cava, R. (2007). Effect of Iberian x Duroc genotype on dry-cured loin quality. Meat Science, 76, 333–341.

Reyes, C., Durán, M.L., Alonso, T., Rodríguez, P.G. and Caro, A. (2008). Behaviour of texture features in a CBIR system. Lecture Notes in Artificial Intelligence, 5271, 425-432.

Siew, L.H., Hodgson, R.M., and Wood, E.J. (1988). Texture measures for carpet wear assessment. IEEE Transactions on Pattern Analysis and Machine Intelligence, 10(1), 92-104.

Sonka, M., Hlavac, V., and Boyle, R. (1999). Image Processing, Analysis, and Machine Vision. Ed. International Thomsom Publishing ITP, Stanford, Connecticut, U.S.A.

Toldrá, F., Flores, M. and Sanz, Y. (1997). Dry-cured ham flavour: enzymatic generation and process influence. Food Chemistry, 59, 523-530.

Utrilla, M.C., Soriana, A. and García Ruiz, A. (2010). Quality attributes of pork loin with different levels of marbling from Duroc and Iberian cross. Journal of Food Quality, 33, 802-820.

Venkatramana, R.B.D. and Jayachandra, P.T. (2010). Colour-Texture image segmentation using Hypercomplex Gabor analysis. Signal & Image Processing: An International Journal, 1(2), 75-86.

Figure Captions

Figure 1. Experimental design

Figure 2. Interpolation and 3D reconstruction of MRI from different acquisition sequences

Figure 3. Adaptation of computational texture algorithms from 2D (a) to 3D images (b)

Figure 1

Figure 1. General procedure.

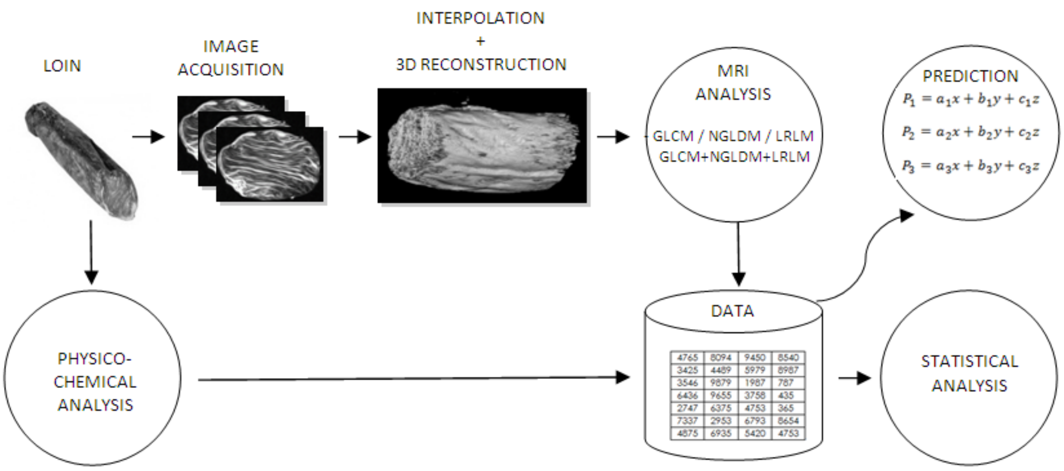

Figure 2

Figure 2: Interpolation and 3D reconstruction of MRI images from different acquisition sequences.

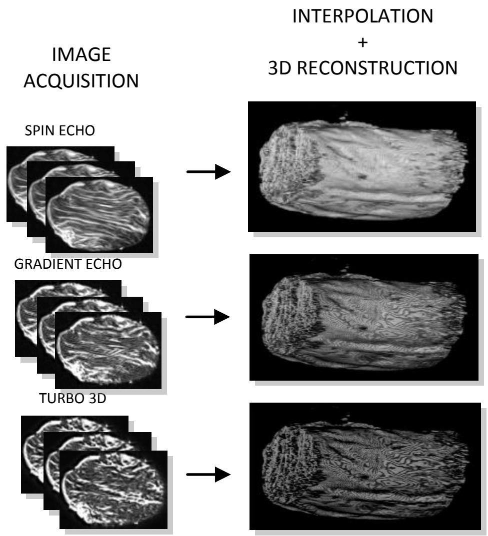

Figure 3

Figure 3: Adaptation of computational texture algorithms from 2D (a) to 3D images (b).

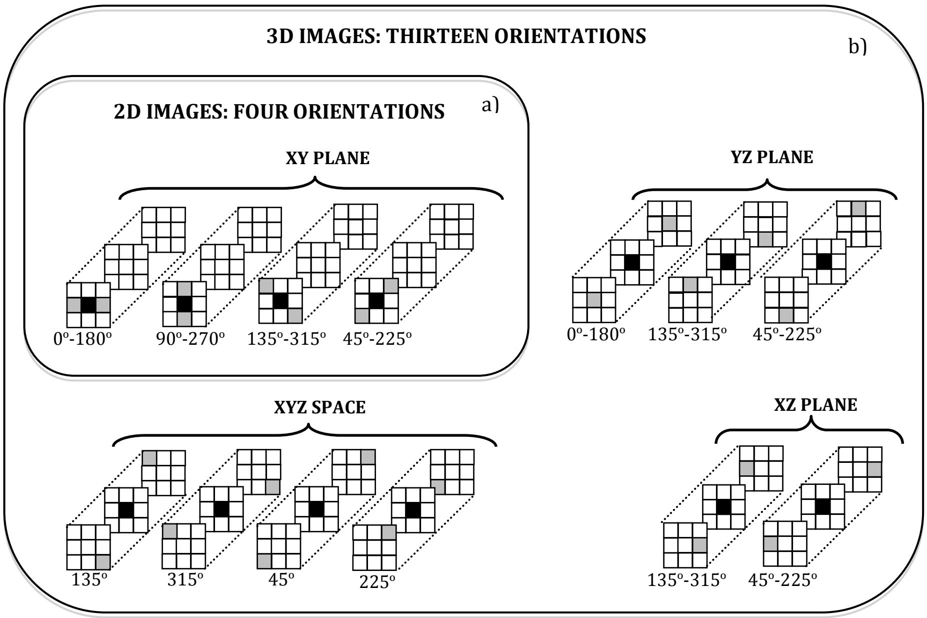

Table 1

Table 1. Parameters for each configuration of the different acquisition sequences: SE (spin echo), GE (gradient echo) and T3D (turbo 3D).

Sequence	Conf.	TE (ms)	TR (ms)	NA	FA	NIm	Thick (ms)	FOV (mm)	FOH
SE	1	26	630	3	n/a	29	4	150x150	None
	2	18	900	3	n/a	29	4	150x150	None
	3	34	630	3	n/a	29	4	150x150	None
	4	26	630	3	n/a	29	4	150x150	None
	5	26	630	1	n/a	29	4	150x150	None
	6	26	630	5	n/a	29	4	150x150	None
	7	26	630	3	n/a	29	4	150x150	High
	8	26	630	3	n/a	29	4	150x150	Low
GE	1	14	1450	7	75	29	4	160x160	None
	2	14	1450	9	75	29	4	160x160	None
	3	14	1800	7	75	29	4	160x160	None
	4	14	800	7	75	29	4	160x160	None
	5	14	2500	7	10	29	4	160x160	None
	6	14	1450	7	90	29	4	160x160	None
	7	14	1450	7	75	29	4	160x160	High
	8	14	1450	7	75	29	4	160x160	Low
T3D	1	16	38	2	65	122	1.1	180x180x140	None
	2	8	38	2	65	122	1.1	180x180x140	None
	3	24	51	2	65	122	1.1	180x180x140	None
	4	8	25	2	65	122	1.1	180x180x140	None
	5	16	120	2	65	122	1.1	180x180x140	None
	6	16	38	2	10	122	1.1	180x180x140	None
	7	16	38	4	10	122	1.1	180x180x140	None
	8	16	38	2	65	122	1.1	180x180x140	Low
	9	16	38	2	90	122	1.1	180x180x140	None
	10	16	38	2	65	122	1.1	180x180x140	High
	11	16	38	2	65	122	1.1	180x180x1v.40	Low

Conf. = Configurations; TE = Echo Time; TR = Repetition Time; NA = Number of Acquisitions; FA = Flip Angle; NIm = Number of Images; Thick = Thickness; FOV = Field Of View; FOH = Filter Of Hamming; n/a = not applicable.

Table 2

Table 2. Normalized values of the 3D computational texture features (from three adapted algorithms) of the MRI of loins acquired with spin echo, gradient echo and Turbo 3D sequences.

	FEATURES	SPIN ECHO	GRADIENT ECHO	TURBO 3D	p
GLCM	Energy	0.2866	0.0924	0.0352	< 0.001
	Entropy	0.4374	0.6093	0.7264	< 0.001
	Correlation	0.2409	0.0441	0.0214	< 0.001
	HC	0.6118	0.6540	0.5546	0.010
	IDM	0.4270	0.2502	0.1965	< 0.001
	Inertia	0.1159	0.1988	0.3248	< 0.001
	CS	0.3365	0.3849	0.4558	< 0.001
	CP	0.0665	0.1849	0.3115	< 0.001
	Contrast	0.5734	0.5949	0.5045	0.026
	Dissimilarity	0.2436	0.3567	0.4638	< 0.001
NGLDM	SNE	0.5096	0.4581	0.7892	< 0.001
	LNE	0.2688	0.0839	0.0777	< 0.001
	NNU	0.5068	0.2874	0.7197	< 0.001
	SM	0.4162	0.2090	0.2452	< 0.001
	ENT	0.4100	0.6775	0.5610	< 0.001
GLRLM	LRE	0.6559	0.3938	0.6294	< 0.001
	SER	0.2099	0.4841	0.2093	< 0.001
	GLNU	0.6394	0.2820	0.8796	< 0.001
	RLNU	0.4621	0.4484	0.7924	< 0.001
	RPC	0.7660	0.5817	0.9311	< 0.001
	GLRE	0.4254	0.1782	0.2462	< 0.001
	HGRE	0.4334	0.5533	0.3747	< 0.001
	SRLGE	0.0532	0.0644	0.1138	0.005
	SRHGE	0.4254	0.5672	0.3891	< 0.001
	LRLGE	0.3597	0.1386	0.1726	< 0.001
	LRHGE	0.4434	0.4165	0.2667	< 0.001

Table 3

Table 3. Correlation coefficient (R) and mean absolute error (MAE) of the prediction equations for physico-chemical parameters of loin obtained by multiple linear regression (MLR), as function of 3D computational texture features algorithms from different sequences of MRI acquisition (spin echo: SE, gradient echo: GE, turbo 3D: T3D).

			GLCM/MAE	**NGLDM**/MAE	**GLRLM**/MAE	**GLCM** **NGLDM**/MAE **GLRLM**
Moisture		SE	**0.931** / 4.090	**0.978** / 2.898	**0.948** / 3.808	**0.978** / 2.601
		GE	**0.965** / 3.234	**0.882** / 5.254	**0.975** / 2.704	**0.976** / 2.198
		T3D	**0.796** / 7.247	**0.632** / 9.325	**0.734** / 7.685	**0.739** / 8.208
Water activity		SE	**0.956** / 0.013	**0.975** / 0.011	**0.945** / 0.014	**0.959** / 0.010
		GE	**0.971** / 0.010	**0.853** / 0.020	**0.972** / 0.010	**0.974** / 0.007
		T3D	**0.795** / 0.026	**0.635** / 0.033	**0.742** / 0.029	**0.724** / 0.031
Lipid		SE	**0.639** / 4.265	**0.718** / 3.711	**0.823** / 3.061	**0.908** / 2.182
		GE	**0.765** / 3.235	**0.627** / 4.112	**0.603** / 3.974	**0.852** / 2.521
		T3D	**0.649** / 3.633	**0.542** / 3.891	**0.505** / 3.838	**0.603** / 3.766
Salt		SE	**0.946** / 0.288	**0.968** / 0.249	**0.945** / 0.308	**0.987** / 0.165
		GE	**0.962** / 0.271	**0.850** / 0.458	**0.970** / 0.226	**0.972** / 0.173
		T3D	**0.784** / 0.589	**0.635** / 0.738	**0.718** / 0.706	**0.683** / 0.717
Color	L*	SE	**0.906** / 2.847	**0.709** / 4.373	**0.919** / 2.630	**0.924** / 2.381
		GE	**0.835** / 3.358	**0.692** / 4.093	**0.874** / 3.245	**0.855** / 3.354
		T3D	**0.629** / 5.042	**0.602** / 4.638	**0.574** / 5.326	**0.642** / 4.899
	a*	SE	**0.820** / 0.941	**0.835** / 0.774	**0.854** / 0.784	**0.924** / 0.572
		GE	**0.842** / 0.857	**0.673** / 1.233	**0.712** / 1.105	**0.779** / 0.994
		T3D	**0.734** / 0.991	**0.444** / 1.305	**0.562** / 1.218	**0.665** / 1.081
	b*	SE	**0.733** / 0.832	**0.744** / 0.850	**0.771** / 0.804	**0.686** / 0.941
		GE	**0.823** / 0.787	**0.680** / 0.908	**0.726** / 0.835	**0.810** / 0.820
		T3D	**0.653** / 0.959	**0.380** / 1.109	**0.517** / 1.008	**0.575** / 0.995

Table 4

Table 4. Correlation coefficient (R) and mean absolute error (MAE) of the prediction equations for physico-chemical parameters of loin obtained by isotonic regression (IR), as function of 3D computational textures feature algorithms from different sequences of MRI acquisition (spin echo: SE, gradient echo: GE, turbo 3D: T3D).

			GLCM/MAE	**NGLDM**/MAE	**GLRLM**/MAE	**GLCM NGLDM GLRLM** /MAE
Moisture		SE	**0.993** / 1.444	**0.993** / 1.543	**0.904** / 3.333	**0.993** / 1.503
		GE	**0.989** / 2.009	**0.891** / 3.204	**0.906** / 3.712	**0.989** / 2.009
		T3D	**0.881** / 4.179	**0.623** / 10.145	**0.782** / 6.756	**0.881** / 4.179
Water activity		SE	**0.994** / 0.004	**0.994** / 0.005	**0.954** / 0.008	**0.994** / 0.004
		GE	**0.995** / 0.004	**0.874** / 0.013	**0.916** / 0.008	**0.995** / 0.004
		T3D	**0.872** / 0.015	**0.522** / 0.041	**0.791** / 0.011	**0.872** / 0.015
Lipid		SE	**0.751** / 3.003	**0.730** / 3.095	**0.654** / 3.567	**0.727** / 3.136
		GE	**0.880** / 2.301	**0.910** / 2.105	**0.554** / 4.160	**0.702** / 3.298
		T3D	**0.675** / 3.317	**0.564** / 3.745	**0.551** / 3.739	**0.675** / 3.317
Salt		SE	**0.998** / 0.051	**0.997** / 0.061	**0.954** / 0.138	**0.998** / 0.051
		GE	**0.998** / 0.043	**0.860** / 0.270	**0.921** / 0.204	**0.998** / 0.043
		T3D	**0.869** / 0.285	**0.561** / 0.847	**0.791** / 0.496	**0.869** / 0.285
Color	L*	SE	**0.915** / 2.207	**0.880** / 3.004	**0.942** / 1.908	**0.915** / 2.210
		GE	**0.842** / 3.250	**0.695** / 3.925	**0.828** / 3.104	**0.842** / 3.250
		T3D	**0.745** / 3.925	**0.340** / 5.975	**0.660** / 4.925	**0.745** / 3.925
	a*	SE	**0.862** / 0.627	**0.802** / 0.743	**0.739** / 0.907	**0.798** / 0.724
		GE	**0.936** / 0.448	**0.933** / 0.470	**0.629** / 1.205	**0.933** / 0.471
		T3D	**0.724** / 0.938	**0.652** / 1.061	**0.614** / 1.109	**0.724** / 0.938
	b*	SE	**0.749** / 0.825	**0.723** / 0.848	**0.684** / 0.945	**0.749** / 0.749
		GE	**0.782** / 0.831	**0.823** / 0.753	**0.643** / 1.044	**0.782** / 0.831
		T3D	**0.705** / 0.862	**0.464** / 1.048	**0.587** / 0.978	**0.705** / 0.862

Table 5

Table 5. Prediction equations for physico-chemical parameters of loins obtained by applying isotonic regression on 3D computational texture features from GLCM of MRI images acquired by gradient echo sequences.

	Moisture =	$1E\text{-}08 * IDM^{6} - 4E\text{-}06 * IDM^{5} + 0{,}0006 * IDM^{4} - 0{,}045 * IDM^{3} + 1{,}7593 * IDM^{2} - 35{,}188 * IDM + 282{,}21$
	Water activity =	$-120{,}49 * IDM^{2} + 227{,}2 * IDM - 106{,}15$
	Lipid =	$0{,}0009 * HC^{4} - 0{,}1103 * HC^{3} + 5{,}0511 * HC^{2} - 98{,}099 * HC + 662{,}09$
	Salt =	$1{,}5734 * CS^{6} + 214{,}18 * CS^{5} - 3627{,}4 * CS^{4} + 21959 * CS^{3} – 58395 * CS^{2} + 57959 * CS - 0{,}0425$
Color	***L* =***	$-9E\text{-}07 * HC^{6} + 0{,}0002 * HC^{5} - 0{,}0286 * HC^{4} + 1{,}7359 * HC^{3} - 58{,}586 * HC^{2} + 1043{,}7 * HC - 7666{,}7$
	a* =	$-0{,}0204 * Energy^{5} + 1{,}4142 * Energy^{4} - 39{,}227 * Energy^{3} + 543{,}34 * Energy^{2} - 3759{,}1 * Energy + 10396$
	b* =	$0{,}1136 * Energy^{6} - 4{,}7197 * Energy^{5} + 81{,}058 * Energy^{4} - 736{,}67 * Energy^{3} + 3736{,}2 * Energy^{2} – 10026 * Energy + 11125$

Table 6

Table 6. Validation of the prediction equations by statistical comparison between real and predicted values for the physico-chemical parameters of fresh and dry-cured loins.

	Fresh loin			**Dry-cured loin**		
	Real	Predicted	***p***	Real	Predicted	***p***
Moisture (%)	65.53	64.55	**0.239**	32.26	33.08	**0.238**
Water activity (%)	0.98	0.98	**0.082**	0.86	0.86	**0.173**
Lipid (%)	12.77	13.31	**0.213**	21.61	21.16	**0.713**
Salt (%)	-	-		2.67	2.60	**0.121**
L	55.33	54.81	**0.321**	40.61	41.05	**0.64**
*a**	12.30	12.43	**0.354**	15.31	15.20	**0.716**
*b**	5.58	5.66	**0.558**	8.05	7.98	**0.77**